arXiv:1402.2280v1 [astro-ph.CO] 10 Feb 2014

Galaxy luminosity function and Tully-Fisher relation: reconciled through rotation-curve studies

Andrea Cattaneo[1], Paolo Salucci[2], & Emmanouil Papastergis[3]

ABSTRACT

The relation between galaxy luminosity L and halo virial velocity $v_{\rm vir}$ required to fit the galaxy luminosity function differs from the observed Tully-Fisher relation between L and disc speed $v_{\rm rot}$. Hence the problem of reproducing the galaxy luminosity function and the Tully-Fisher relation simultaneously has plagued semianalytic models since their inception. Here we study the relation between $v_{\rm rot}$ and $v_{\rm vir}$ by fitting observational average rotation curves of disc galaxies binned in luminosity. We show that the $v_{\rm rot}$- $v_{\rm vir}$ relation that we obtain in this way can fully account for this seeming inconsistency. Therefore, the reconciliation of the luminosity function with the Tully-Fisher relation rests on the complex dependence of $v_{\rm rot}$ on $v_{\rm vir}$, which arises because the ratio of stellar mass to dark matter mass is a strong function of halo mass.

1. Introduction

In the standard ΛCDM cosmology, $\sim 84\%$ of the mass of the Universe is composed of dark matter (DM), which dominates gravitational evolution on large scales. Galaxies are baryonic condensations at the centres of DM haloes formed by gravitational instability of primordial density fluctuations. The main goal for studies of galaxy formation in a cosmological context is to explain the properties of galaxies (luminosities, spectra, sizes, and morphologies) in terms of the growth histories of their host haloes.

Historically, the main observational constraints on the link between luminous galaxies and the underlying DM distribution come from the galaxy luminosity function (LF) and

[1]Laboratoire d'Astrophysique de Marseille, UMR 6110 CNRS, Univ. d'Aix-Marseille, 38 rue F. Joliot-Curie, 13388 Marseille cedex 13, France, *r-mail:* andrea.cattaneo@oamp.fr

[2]Department of Astrophysics, SISSA, Via Beirut, 2-4, 34014 Trieste, Italy, *e-mail:* salucci@sissa.it

[3]Center for Radiophysics and Space Research, Space Sciences Building, Cornell University, Ithaca, NY 14853, USA, *e-mail:* papastergis@astro.cornell.edu

from the Tully-Fisher (TF) relation $L \propto v_{\rm rot}^{\eta}$ that links the luminosity L of a disc galaxy and its reference speed $v_{\rm rot}$ ($\eta \sim 3-4$ depending on the band. Fig. 1 shows the I-band TF relation of Yegorova & Salucci 2007). Today, there are further constraints from weak lensing data (Mandelbaum et al. 2006; Leauthaud et al. 2010; Reyes et al. 2012), velocity dispersion profiles (Martinsson et al. 2013) [1], and kinematics of satellite galaxies (Conroy et al. 2007; More et al. 2011). The latter probe the gravitational potential of spiral galaxies at large radii. Yegorova et al. (2011) find that their results are consistent with those from rotation-curve (RC) data in a statistical sense.

The importance of the LF and the TF relation for constraining the relation between galaxy luminosity and halo mass is readily explained. Let us start from the LF. If a volume of the universe contains n haloes of mass M_h, and if each halo of mass M_h hosts a galaxy of luminosity L, then the volume must contain n galaxies with luminosity L. More generally, the number of galaxies brighter than L in a given band must be equal to the number of haloes more massive than M_h if L is a growing function of M_h - a general predictions of galaxy formation models and simulations in bands where luminosity traces stellar mass. The LF of galaxies is observed and the ΛCDM model makes strong predictions for the mass function of DM haloes. Hence, there is a well defined $L - M_h$ relation that cosmological models must satisfy to fit the galaxy LF. It is straightforward to convert this relation into a relation between L and $v_{\rm vir}$ by using the fitting formulae of Bryan & Norman (1998) for the virial overdensity contrast.

The black dashed curve in Fig. 1 shows the $L - v_{\rm vir}$ relation that we obtain when we apply this method to the LF of Papastergis et al. (2012) and to the halo mass function for a ΛCDM cosmology with $h_0 = 0.73$, $\Omega_m = 0.24$, $\Omega_\Lambda = 0.76$, $\sigma_8 = 0.76$. The I-band LF of Papastergis et al. (2012) is constructed by computing the Kron-Cousin I-band magnitude of each individual galaxy from its SDSS r- and i-band magnitudes. We have verified that this LF is consistent with the SDSS DR6 i-band LF of Montero-Dorta & Prada (2009) when we convert the latter to I band by using mean $I - i$ colours in Fukugita et al. (1995). The halo mass function comes a cosmological N-body simulation that was run by the Horizon Project (`http://www.projet-horizon.fr`) and is the same that we used in Papastergis et al. (2012), to whom we refer for all details concerning the abundance matching procedure.

Let us now consider the TF relation. The disc rotation speed $v_{\rm rot}(r)$ measures the total

[1] One can measure the absorption lines of disc stars at some height z over the disc and derive a stellar velocity dispersion profile, which can be used for global mass modelling. This method is in principle very useful, especially for spirals in which the rotation curves (RCs) alone are not sufficient for it. In practice, recent work (Martinsson et al. 2013) shows that this technique is not yet able to give a unique luminous-DM decomposition but that, coupled with other determinations, it can be decisive to improve their accuracy.

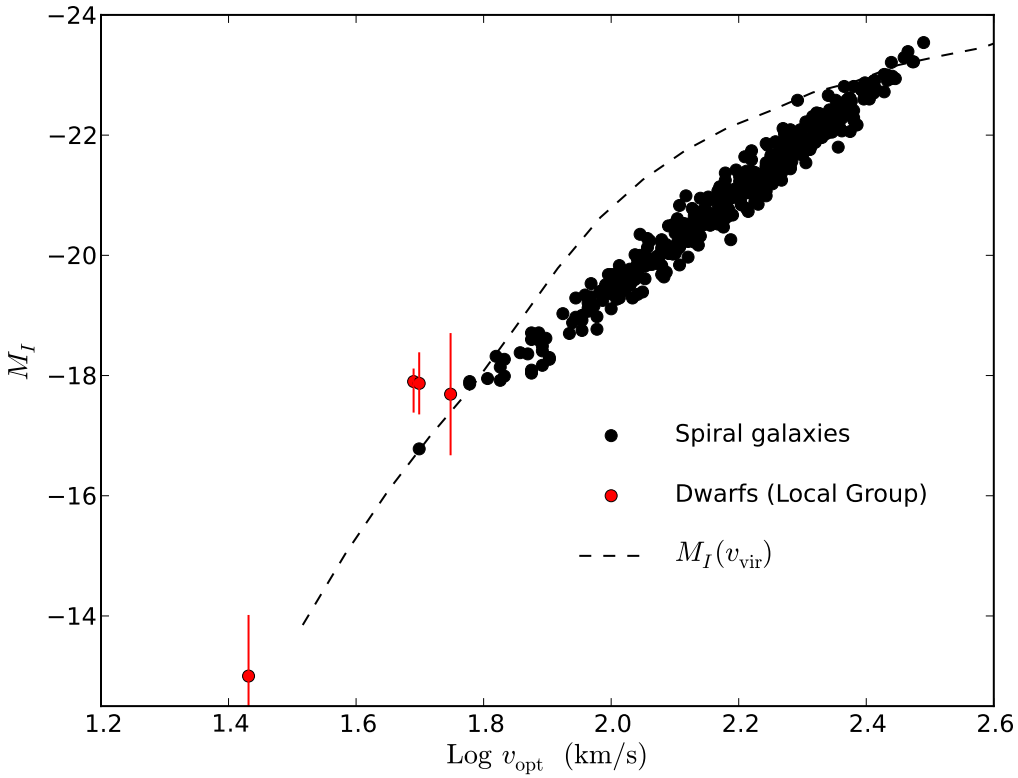

Fig. 1.— Black symbols: the TF relation for the spiral-galaxy sample of Yegorova & Salucci (2007). M_I is the absolute magnitude in the I-band of Kron-Cousin, $v_{\rm opt}$ is the speed at the optical radius (equal to 3.2 exponential radii). Red symbols: four dwarf galaxies from Salucci et al. (2012) inserted to extend the TF relation to $M_I \sim -13$. Black dashed curve: the L_I - $v_{\rm vir}$ relation that we obtain by matching the Kron-Cousin I-band LF of Papastergis et al. (2012) and the halo mass function from a cosmological simulation with $h_0 = 0.73$, $\Omega_m = 0.24$, $\Omega_\Lambda = 0.76$, and $\sigma_8 = 0.76$.

mass M within radius r, which is dominated by DM for large values of r. Since, at large radii, the RCs of disc galaxies are nearly flat, the TF relation implies a relation between L and $v_{\rm vir}$. The trouble is that this relation differs from the one that we find from the LF.

Fig. 1 illustrates the problem by comparing the $L_I - v_{\rm vir}$ relation that we derive from abundance matching (black dashed line) with the I-band TF relation of Yegorova & Salucci (2007, black symbols). This discrepancy cannot be attributed to variations in mass-to-light ratio because the entire analysis has been done using the Kron-Cousin I-band luminosity both for the LF and the TF relation. This is a strong point of our work and the reason why Fig. 1 is totally independent of any assumption on the stellar mass-to-light ratio (on the issue of mass-to-light ratios, also see Dwarf spheroidal galaxy kinematics and spiral galaxy scaling laws por).

The discrepancy shown in Fig. 1 has been known for twenty years and is independent of the abundance-matching method because any model that matches the galaxy LF ends up with an $L_I - v_{\rm vir}$ relation similar to the black dashed line. Either models are calibrated on the TF relation and fail to fit the LF (Kauffmann et al. 1993) or they are calibrated on the LF and they fail to reproduce the TF relation (Heyl et al. 1995). This inconsistency has plagued galaxy formation models since the earliest studies. The discrepancy persists today (Guo et al. 2010).

Dutton et al. (2010) and Reyes et al. (2012) have recently pointed that the problem derives from the incorrect assumption that $v_{\rm rot}$ is a good tracer of $v_{\rm vir}$. Dutton et al. (2010) used different methods (satellite kinematics, weak lensing observations, abundance matching) to investigate the halo masses of early- and late-type galaxies and compared the stellar mass - virial velocity relations derived from these studies with the Faber-Jackson and the TF relation. They found that the disc rotation speed $v_{\rm rot}$ and the virial velocity $v_{\rm vir}$ are systematically different and that $v_{\rm rot}/v_{\rm vir}$ varies with stellar mass. Reyes et al. (2012) did the same type analysis for a galaxy sample for which they had both the TF relation and weak lensing data. Their results are in qualitative agreement with Dutton et al. (2010), though their values of $v_{\rm rot}/v_{\rm vir}$ are systematically higher.

Our article follows the same general philosophy of these two previous studies but the method is completely different because first we determine $v_{\rm rot}/v_{\rm vir}$ as a function of L_I from the modelling of disc RCs and then we use this result to convert the $L_I - v_{\rm vir}$ relation from abundance matching into a relation between L_I and $v_{\rm rot}$, which can be compared with the TF relation. The originality of the article is that, following Salucci et al. (2007), we compute the $v_{\rm rot}/v_{\rm vir}$-L_I with a method that is completely independent of the galaxy LF *and* we find that this relation is precisely the one we need to reconcile the TF relation with the galaxy LF.

The structure of the article is as follows. In Section 2, we present our RC analysis and our results for the $v_{\rm rot}$-$v_{\rm vir}$ relation. In Section 3, we combine the results of the previous section with those from abundance matching to compute a TF that will be found to be in agreement with the observations, and we discuss the significance of this final result.

2. The relation between $v_{\rm opt}$ and $v_{\rm vir}$

Our method to compute $v_{\rm vir}$ is conceptually quite simple. We fit the RCs of spiral galaxies by assuming that they are made of two components: a baryonic disc and a DM halo. The best-fit DM-halo profile is extrapolated out the radius $r_{\rm vir}$ where the mean density equals the critical density of the Universe times the virial overdensity contrast computed with the formulae by Bryan & Norman (1998). The virial velocity $v_{\rm vir}$ is equal to the circular velocity at this radius. In practice, to apply this method, we need to specify three things: a model for the density distribution of the baryonic disc, a model for the density distribution of the DM haloes, and the RCs on which we intend to do the analysis. Let us analyse these three elements one by one.

2.1. The baryonic disc model

We model the baryonic disc with a single exponential profile. This model contains two parameters: the total disc mass M_d (stars plus gas) and the disc exponential radius r_d. We do not treat r_d as a free parameter of the fit. Instead, we require it to be equal to the exponential radius of the I-band surface-brightness profile. This is equivalent to assuming that the gas and the stellar disc have the same scale-length. In fact, the gas distribution is usually more extended, but this has almost no effect on our results for the following reason. Small galaxies are completely DM-dominated. An error on the spatial extension of the baryonic component will have little effect on the best-fit parameters for the dominant DM component (this point is shown quantitatively in Persic et al. 1996). In massive galaxies, the baryonic component is dynamically important, but these galaxies have low gas fractions. Therefore, the gas component has a negligible effect on the size of the baryonic disc.

2.2. The dark matter halo model

Cosmological simulations of dissipationless hierarchical clustering in a cold DM Universe find that the density distribution of DM haloes are described by the NFW (Navarro et al.

1997) profile:

$$\rho(r) = \frac{\rho_0}{\frac{r}{r_0}\left(1+\frac{r}{r_0}\right)^2}, \tag{1}$$

with concentration

$$c(M_{\rm vir}) = \frac{r_{\rm vir}}{r_0} = 9.6\left(\frac{M_{\rm vir}}{10^{12}h^{-1}M_\odot}\right)^{-0.075} \tag{2}$$

for haloes at $z \simeq 0$ (Klypin et al. 2011). This profile provides a poor fit to the RCs of spiral galaxies in the inner regions (Flores & Primack 1994; and Moore 1994; but also see Swaters et al. 2003).

The Burkert (1995) profile

$$\rho(r) = \frac{\rho_0}{\left(1+\frac{r}{r_0}\right)\left(1+\frac{r^2}{r_0^2}\right)}, \tag{3}$$

gives a much better fit to the observed RCs (Fig. 2), though with concentration-parameter values that are $\sim 1.4-1.5$ times larger than suggested by Eq. (2). As this is is a phenomenological paper, the fact that the Burkert model fits the observation is a good enough reason for using it independently of any theoretical argument. However, some reader may wonder whether it is self-consistent to use the Burkert profile (Eq. 3) alongside the halo mass function from a simulation that assumes a cold DM cosmology. To address this objection, we remark that our choice is justified for two reasons. First, Eq. (1) and Eq. (3) are almost identical at $r \gtrsim r_0$ and differ only at small radii, while here we are interested in the DM density distribution at large radii. Recent hydrodynamical simulations have shown that the difference at small radii may be understood as an effect of supernova feedback, which was not considered in pure N-body simulations (Governato et al. 2010; Pontzen & Governato 2012; Brook et al. 2012; Teyssier et al. 2013). Second, the concentration difference can be explained as being due to adiabatic contraction. We have verified this point quantitatively by comparing the DM density profile in a simulation by Geen et al. (2013) in the cases with pure DM and with baryon cooling.

2.3. The RCs

Our analysis is based on a sample of 967 spiral galaxies for which there are high-quality Hα data and I-band photometry (Persic & Salucci 1995; Mathewson et al. 1992). The sample is split in eleven luminosity bin and each luminosity bin is analysed separately. Instead of analysing the RC of each galaxy individually and then computing an average $v_{\rm rot}/v_{\rm vir}$, we directly analyse the co-added RCs of PSS (Persic et al. 1996), obtained by stacking the RCs

of the galaxies in each bin. Following PSS, the co-added RCs are computed by averaging the values of $v_{\rm rot}$ in bins of $r/r_{\rm opt}$, where $r_{\rm opt} = 3.2r_d$ (r_d is the exponential radius of the I-band surface brightness profile). The points with error bars in Fig. 2 show the co-added RCs in the eleven I-band magnitude bins.

2.4. The fit

In each magnitude bin, we fit the co-added RC with a disc plus halo model (Fig. 2). We do the fit at $0.5 < r/r_{\rm opt} < 2$ to give more weight to the outer regions. The result is generally quite good (compare the solid lines and the points with error bars).

The disc contribution is a strong function of luminosity. Faint galaxies ($M_I \gtrsim 19$) are entirely DM-dominated. Their RCs rise steeply out to $r = 2r_{\rm opt}$. Bright spirals ($M_I < -22$) are disc dominated out to very large radii. Their RCs peak at $0.5 < r/r_{\rm opt} < 1$ and decrease at larger radii.

Let $v_{\rm opt}$ be the mean rotation speed at the optical radius and let $v_{\rm vir}$ be the virial velocity obtained for the best-fit halo parameter by extrapolating the halo contribution out the virial radius (the radius within which the mean density equals the critical density of the Universe times the critical overdensity contrast computed with the fitting formulae of Bryan & Norman 1998). By computing $v_{\rm opt}$ and $v_{\rm vir}$ for each of our magnitude bins, we obtain the $v_{\rm opt}$ - $v_{\rm vir}$ relation that is shown by the red solid curve in Fig. 3.

Fig. 3 shows that $v_{\rm opt}$ differs from $v_{\rm vir}$. The difference is by a factor of ~ 1.3 but its precise value varies with $v_{\rm vir}$ and has a maximum of $v_{\rm opt}/v_{\rm vir} \sim 1.5$ for $v_{\rm vir} \sim 100\,{\rm km\,s^{-1}}$. This result is consistent with the one from weak lensing by Reyes et al. (2012) when we correct for the difference in our definition of $r_{\rm vir}$. Dutton et al. (2010) find a curve $v_{\rm rot}/v_{\rm vir}$ vs. $v_{\rm vir}$ with the same shape and the maximum in the same position but their values of $v_{\rm rot}/v_{\rm vir}$ are systematically lower (their maximum value for $v_{\rm rot}/v_{\rm vir}$ is closer to 1.1).

In Fig. 3, we have also compared our results to those obtained with the abundance-matching method by Papastergis et al. (2011) (solid blue curve; the same approach has also been explored by Trujillo-Gomez et al. 2011). Papastergis et al. (2011) have considered the galaxy velocity function computed by using the HI rotation speed for disc galaxies and $\sigma\sqrt{2}$ for elliptical galaxies where σ is the stellar velocity dispersion at 1/8 effective radii and they have matched this velocity function to the virial velocity function of DM haloes. Given that the two methods are totally unrelated, the broad agreement of the red curve and the blue curve is quite significant. Furthermore, a small deviation is not unexpected, since rotation speeds measured from the width of the HI line are generally slightly larger than $v_{\rm opt}$

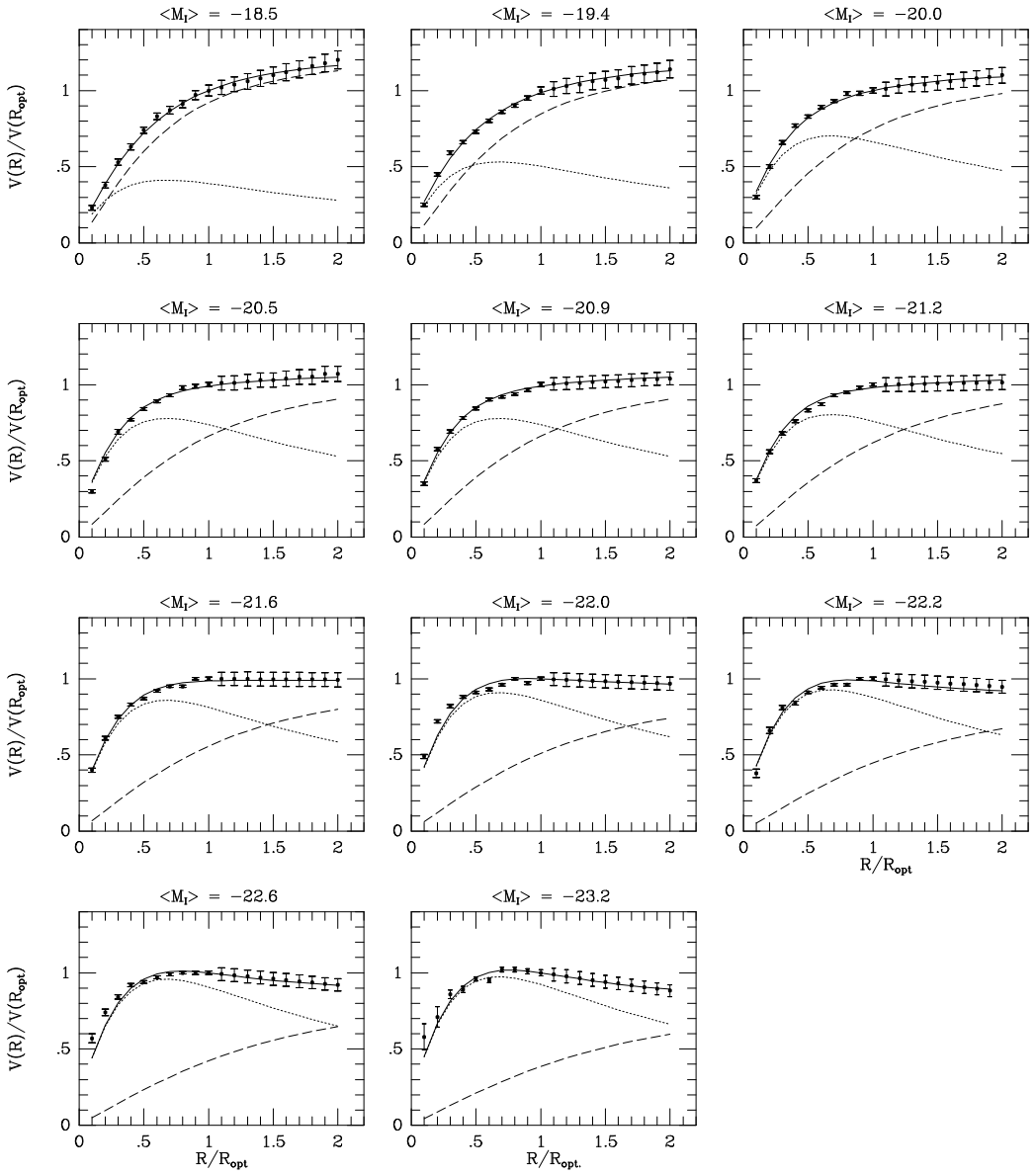

Fig. 2.— Points with error bars: the co-added RCs in eleven I-band magnitude bins for the 967 spiral galaxies in PSS's sample. Curves: each co-added RC is fitted with a disc (dotted curve) and a halo (dashed curve) contribution. Their sum is shown by the solid curve. Faint spirals are dark-matter dominated at all radii. Bright spirals are disc-dominated at all radii.

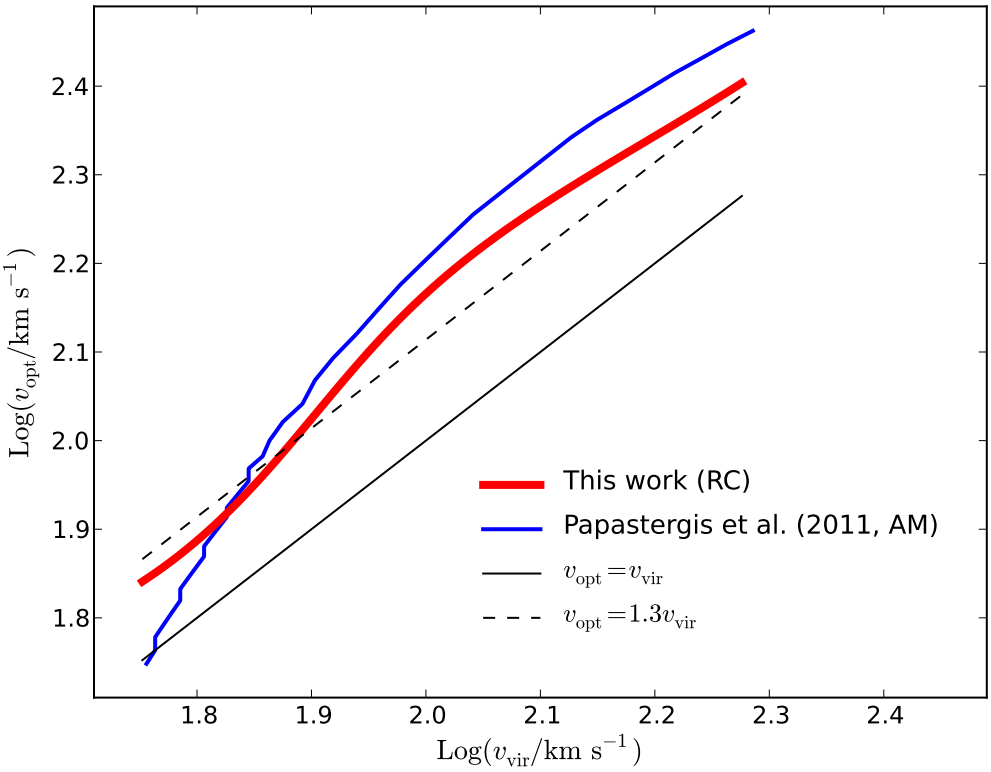

Fig. 3.— Thick red curve: the $v_{\rm opt}$ - $v_{\rm vir}$ relation that we obtain from our rotation curve (RC) analysis. Blue curve: the $v_{\rm opt}$ - $v_{\rm vir}$ that Papastergis et al. (2011) obtained with the abundance matching (AM) method by matching the galaxy velocity function and the halo virial velocity function. Thin black solid line: the relation that one would have if $v_{\rm opt} = v_{\rm vir}$ (shown for comparison). Thin black dashed line: the relation that one would have if $v_{\rm opt} = 1.3v_{\rm vir}$ (shown for comparison).

(Dutton et al. 2010).

Finally, we recall that, in Tonini et al. (2006), we had computed the spin parameter of spiral galaxies by using PSS's universal RC (automatically in agreement with the TF relation) in conjunction with the disc - halo mass relation from abundance matching (also see Shankar et al. 2006). Our article shows that the approach of these studied was well grounded.

3. LF and TF relation: reconciled at last

In Section 2, we have used our analysis of disc RCs to determine the relation between $v_{\rm rot}$ and $v_{\rm vir}$ (the red curve in Fig. 3). Now, we use this relation to transform the M_I - $v_{\rm vir}$ relation from abundance matching (the dashed curve in Fig. 1) into a relation between M_I and $v_{\rm opt}$. This relation is shown by the red curve in Fig. 4 and is in excellent agreement with the TF data points (black symbols; they are the same in Fig. 1 and Fig. 4). Our conclusion is that we do not encounter any problem at reproducing the LF and the TF relation simultaneously when the dependence of $v_{\rm opt}$ on $v_{\rm vir}$ is properly accounted for.

Our result is established in the magnitude range $-22 < M_I < -18$. LF data (from which we derive the dashed curve in Fig. 1) exist down to $M_I \sim -14$ but we still lack a statistically significant dwarf-galaxy sample with high-quality RCs that may allow us to extend our analysis at $M_I > -18$, although progress in this direction is being made (e.g. the 30-galaxy sample by Martinsson et al. 2013). Even with these uncertainties, there is evidence that the TF relation may bend at low luminosities (e.g. Trujillo-Gomez et al. 2011 and our lowest-luminosity dwarf-galaxy data point).

The quality of the agreement at $-22 < M_I < -18$ is also linked to the consistency of our procedure. The $v_{\rm opt}/v_{\rm vir}$ that we use to pass from $v_{\rm vir}$ to $v_{\rm opt}$ is measured from the same RCs from which we extract the TF data points. Furthermore, our choice to work with I-band luminosity throughout the article, both for the LF and TF relation, avoids introducing the uncertainty of stellar mass-to-light ratios

At high luminosities, the red curve shows a hint of flattening, which is not seen in TF data points, but this happens because the abundance-matching relation (the black dashes) is computed from the total LF, which is dominated by early-type galaxies at high luminosity, while TF relation is shown for spiral galaxies only. The implication is that, for a same $v_{\rm vir}$, spiral galaxies have a higher I-band luminosity than elliptical ones. This result is in agreement with Trujillo-Gomez et al. (2011), and also with Wojtak & Mamon (2013), who find that, for a same $M_{\rm halo}$, late-type galaxies have higher $M_\star/M_{\rm halo}$, where $M_\star$ is the stellar

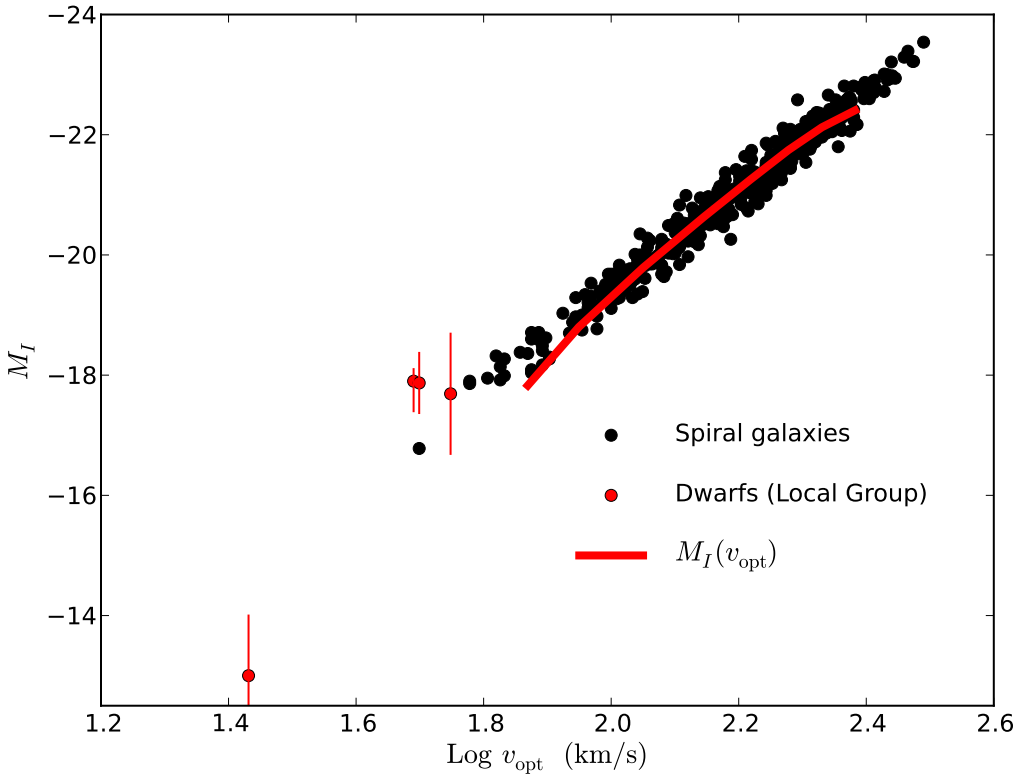

Fig. 4.— Black symbols: TF data points (same as in Fig. 1). Red symbols: four dwarf galaxies inserted to extend the TF relation to $M_I \sim -13$ (same as in Fig. 1). Red curve: the result of converting the M_I-$v_{\rm vir}$ relation (the dashed line in Fig. 1) into an M_I-$v_{\rm opt}$ relation by using the $v_{\rm rot}$-$v_{\rm vir}$ relation that we extract from our analysis of observed rotation curves (the red curve in Fig. 3).

mass. Dutton et al. 2010 reach the same conclusion when making the comparison at a fixed $M_\star$

The dependence of $v_{\rm opt}/v_{\rm vir}$ on $v_{\rm vir}$ is of paramount importance to explain how it is possible to reconcile TF relation (a single power-law) with the LF, which has a break at the characteristic luminosity $L_\star$. This dependence arises from the strong trend in $M_\star/M_{\rm halo}$ with halo mass. This can be seen both through the disc/halo decomposition of the RCs (PSS) and through the results of abundance matching, stellar-kinematics, and weak-lensing studies (see Papastergis et al. 2012, where we also compare the results of many different authors).

REFERENCES

Brook C. B., Stinson G., Gibson B. K., Wadsley J., Quinn T., 2012, MNRAS, 424, 1275

Bryan G. L., Norman M. L., 1998, ApJ, 495, 80

Burkert A., 1995, ApJ, 447, L25

Conroy C., Wechsler R. H., Kravtsov A. V., 2007, ApJ, 668, 826

Dutton A. A., Conroy C., van den Bosch F. C., Prada F., More S., 2010, MNRAS, 407, 2

Flores R. A., Primack J. R., 1994, ApJ, 427, L1

Fukugita M., Shimasaku K., Ichikawa T., 1995, "Publ. of the Astron. Soc. of the Pacific", 107, 945

Geen S., Slyz A., Devriendt J., 2013, MNRAS, 429, 633

Governato F., Brook C., Mayer L., Brooks A., Rhee G., Wadsley J., Jonsson P., Willman B., Stinson G., Quinn T., Madau P., 2010, Nature, 463, 203

Guo Q., White S., Li C., Boylan-Kolchin M., 2010, MNRAS, 404, 1111

Heyl J. S., Hernquist L., Spergel D. N., 1995, ApJ, 448, 64

Kauffmann G., White S. D. M., Guiderdoni B., 1993, MNRAS, 264, 201

Klypin A. A., Trujillo-Gomez S., Primack J., 2011, ApJ, 740, 102

Leauthaud A., Finoguenov A., Kneib J.-P., Taylor J. E., Massey R., Rhodes J., Ilbert O., Bundy K., Tinker J., George M. R., Capak P., 2010, ApJ, 709, 97

Mandelbaum R., Seljak U., Kauffmann G., Hirata C. M., Brinkmann J., 2006, MNRAS, 368, 715

Martinsson T. P. K., Verheijen M. A. W., Westfall K. B., Bershady M. A., Andersen D. R., Swaters R. A., 2013, A&A, 557, A131

Mathewson D. S., Ford V. L., Buchhorn M., 1992, ApJS, 81, 413

Montero-Dorta A. D., Prada F., 2009, MNRAS, 399, 1106

Moore B., 1994, Nature, 370, 629

More S., van den Bosch F. C., Cacciato M., Skibba R., Mo H. J., Yang X., 2011, MNRAS, 410, 210

Navarro J. F., Frenk C. S., White S. D. M., 1997, ApJ, 490, 493

Papastergis E., Cattaneo A., Huang S., Giovanelli R., Haynes M. P., 2012, ApJ, 759, 138

Papastergis E., Martin A. M., Giovanelli R., Haynes M. P., 2011, ApJ, 739, 38

Persic M., Salucci P., 1995, ApJS, 99, 501

Persic M., Salucci P., Stel F., 1996, MNRAS, 281, 27

Pontzen A., Governato F., 2012, MNRAS, 421, 3464

Reyes R., Mandelbaum R., Gunn J. E., Nakajima R., Seljak U., Hirata C. M., 2012, MNRAS, 425, 2610

Salucci P., Lapi A., Tonini C., Gentile G., Yegorova I., Klein U., 2007, MNRAS, 378, 41

Salucci P., Wilkinson M. I., Walker M. G., Gilmore G. F., Grebel E. K., Koch A., Frigerio Martins C., Wyse R. F. G., 2012, MNRAS, 420, 2034

Shankar F., Lapi A., Salucci P., De Zotti G., Danese L., 2006, ApJ, 643, 14

Swaters R. A., Verheijen M. A. W., Bershady M. A., Andersen D. R., 2003, ApJ, 587, L19

Teyssier R., Pontzen A., Dubois Y., Read J. I., 2013, MNRAS, 429, 3068

Tonini C., Lapi A., Shankar F., Salucci P., 2006, ApJ, 638, L13

Trujillo-Gomez S., Klypin A., Primack J., Romanowsky A. J., 2011, ApJ, 742, 16

Wojtak R., Mamon G. A., 2013, MNRAS, 428, 2407

Yegorova I. A., Pizzella A., Salucci P., 2011, A&A, 532, A105

Yegorova I. A., Salucci P., 2007, MNRAS, 377, 507

This preprint was prepared with the AAS LaTeX macros v5.2.